

Sorption of beryllium in cementitious systems relevant for nuclear waste disposal: Quantitative description and mechanistic understanding

N. Çevirim-Papaioannou^{a,**}, I. Androniuk^a, S. Han^b, N. Ait Mouheb^{a,1}, S. Gaboreau^c, W. Um^b, X. Gaona^{a,*}, M. Altmaier^a

^a Institute for Nuclear Waste Disposal (INE), Karlsruhe Institute of Technology (KIT), Karlsruhe, Germany

^b Division of Advanced Nuclear Engineering (DANE), Pohang University of Science and Technology (POSTECH), Pohang, Gyeongbuk, South Korea

^c BRGM Bureau de Recherches Géologiques et Minières, Orleans, France

A B S T R A C T

Handling Editor: Milena Horvat

Keywords:

Beryllium
Sorption
Cement
C–S–H phases
Molecular dynamics
Mechanistic understanding

Beryllium has applications in fission and fusion reactors, and it is present in specific streams of radioactive waste. Accordingly, the environmental mobility of beryllium needs to be assessed in the context of repositories for nuclear waste. Although cement is widely used in these facilities, Be(II) uptake by cementitious materials was not previously investigated and was hence assumed negligible.

Sorption experiments were performed under Ar-atmosphere. Ordinary Portland cement, low pH cement, calcium silicate hydrated (C–S–H) phases and the model system TiO₂ were investigated. Sorption kinetics, sorption isotherms and distribution ratios (R_d , in kg·L⁻¹) were determined for these systems. Molecular dynamics were used to characterize the surface processes driving Be(II) uptake.

A strong uptake ($5 \leq \log R_d \leq 7$) is quantified for all investigated cementitious systems. Linear sorption isotherms are observed over three orders of magnitude in [Be(II)]_{aq}, confirming that the uptake is controlled by sorption processes and that solubility phenomena is not relevant within the investigated conditions. The analogous behaviour observed for cement and C–S–H support that the latter are the main sink of beryllium. The two step sorption kinetics is explained by a fast surface complexation process, followed by the slow incorporation of Be(II) in C–S–H. Molecular dynamics indicate that Be(OH)₃⁻ and Be(OH)₂⁰ are sorbed to the C–S–H surface through Ca-bridges.

This work provides a comprehensive quantitative and mechanistic description of Be(II) uptake by cementitious materials, whose retention properties can be now reliably assessed for a wide range of boundary conditions of relevance in nuclear waste disposal.

1. Introduction

Beryllium is used as neutron reflector and moderator in test and research fission reactors due to its specific chemical and structural properties, relatively low neutron absorption cross section and high neutron scattering cross section (Beeston, 1970; Chandler et al., 2009; Longhurst et al., 2003). Beryllium is also considered as a plasma-facing material and neutron multiplication in breeding blankets in fusion reactors (Kawamura et al., 2004; Longhurst et al., 2003). In these applications, substantial amounts of ⁴He, ³He and ³H gases are generated as a

result of (n, 2n) and (n, α) reactions, leading to the swelling of beryllium and to significant changes in its mechanical properties (Chandler et al., 2009; Longhurst et al., 2003). Irradiated beryllium components must be regularly replaced, and thus are part of the inventory in specific wastestreams of nuclear waste to be disposed of in deep underground repositories. The potential release of chemotoxic substances (e.g. Be) and subsequent human exposure is strongly dependent on the waste inventory, repository design, solubility and sorption properties of the chemotoxic substance, exposure pathways, as well as on human intrusion scenarios (Thorne, 2007; Wilson et al., 2009). Although the main

* Corresponding author.

** Corresponding author.

E-mail addresses: nese.cevirim@kit.edu (N. Çevirim-Papaioannou), xavier.gaona@kit.edu (X. Gaona).

¹ Current address: Forschungszentrum Jülich GmbH, Institute of Energy and Climate Research – Nuclear Waste Management and Reactor Safety (IEK-6), Jülich, Germany.

toxicological properties of beryllium are related to inhalation, ingestion pathways related to the possible release of beryllium from the repository to the biosphere need to be taken into account (Thorne, 2007).

The safety concept in underground repositories relies on the combination of engineered and geological barriers, which minimize the release of radionuclides into the biosphere. Cementitious materials are used for the stabilization of the waste and for construction purposes, mostly (but not exclusively) in the case of low- and intermediate level radioactive waste (L/ILW). The contact of cement with groundwater leads to its chemical degradation, which is commonly described in three degradation stages (Atkinson et al., 1988; Berner, 1992; Ochs et al., 2016; J. Tits et al., 2018; Wieland et al., 2003). In the degradation stage I, the composition of the porewater is controlled by the dissolution of K- and Na-oxide/hydroxides, buffering the pH at ≈ 13.3 and leading to high alkali concentrations in solution ($[K^+] \approx 0.18$ M, $[Na^+] \approx 0.11$ M). Degradation stage II is dominated by the dissolution of portlandite, $Ca(OH)_2$, which buffers the pH at ≈ 12.5 and imposes high calcium concentrations in the pore water ($[Ca]_{tot} \approx 2 \cdot 10^{-2}$ M). After the complete dissolution of portlandite, the degradation stage III is characterized by the incongruent dissolution of calcium silicate hydrated (C–S–H) phases. Throughout this process, the Ca:Si ratio of C–S–H phases varies from ≈ 1.6 to ≈ 0.6 , whilst the pH decreases from ≈ 12.5 to ≈ 10 .

Low-pH cement formulations are gaining relevance in the context of nuclear waste disposal due to the negative impact that high-pH plumes can potentially have on other natural or engineered barriers, especially those containing clay materials. In low-pH cements, discussed for potential use in order to limit alkalinity inventories, the addition of materials such as silica fume, blast furnace slag or fly ash to cement results in a low content/absence of portlandite and an increased fraction of C–S–H phases with low Ca:Si ratio (Calvo et al., 2010; Codina et al., 2008; Coumes et al., 2006; Lothenbach et al., 2012; Savage et al., 2007; Vasconcelos et al., 2020).

C–S–H phases are considered as the main sink of several metal ions in cementitious materials. Three main mechanisms are described in the literature for the uptake of metal ions by C–S–H phases: (i) surface complexation onto the silanol groups of the C–S–H surface, (ii) incorporation in C–S–H structure by replacement of Ca^{2+} in the CaO layers, and (iii) development of a bond to the interlayer silandiol groups, which can be also interpreted as incorporation in the C–S–H interlayer (Tits and Wieland, 2018).

In contrast to beryllium, the uptake of other alkali-earth metals by cementitious materials has been extensively investigated in the literature (Bayliss et al., 1989; Dauzeres et al., 2010; Holland et al., 1992; Jenni et al., 2014; Lothenbach et al., 2015; Missana et al., 2017; Olmeda et al., 2019; Tits, Iijima, et al., 2006; Tits, Wieland, et al., 2006; Wieland et al., 2008). Sr(II), Ba(II) and Ra(II) are characterized by a weak to moderate uptake, with distribution coefficients (R_d) ranging from 10 to 10^4 L kg⁻¹. Both surface complexation and ion exchange with Ca are described as main uptake mechanisms for these metals. On the other hand, Mg(II) is known to form magnesium silicate hydrated phases (M–S–H), which are stable in alkaline systems with pH ≈ 8 to ≈ 11 (Dauzeres et al., 2010; Jenni et al., 2014; Lothenbach et al., 2015).

A number of experimental studies available in the literature have investigated the uptake of other divalent metals (e.g. Fe(II), Zn(II), Cd(II), Pb(II), among others) by cement and C–S–H phases (Mancini et al., 2020; Ochs et al., 2002; Pointeau et al., 2001; Pomies et al., 2001; Tommaseo et al., 2002; Ziegler et al., 2001a; Ziegler et al., 2001b). For some of these elements (e.g. Zn(II), Pb(II)), the uptake by cement and C–S–H phases has been reported to decrease with increasing pH. The analogies in the aqueous speciation of these metal ions with Be(II), which involve the predominance of $M(OH)_3$ and $M(OH)_4^{2-}$ hydrolysis species in hyperalkaline systems, may provide relevant insights to understand the uptake of beryllium by cementitious materials.

Aluminium is a relevant element in cementitious systems, where it is predominantly found as calcium aluminate hydrate phases (AFm) and

ettringite (Taylor, 1997). Aluminium is taken up strongly by C–S–H phases, and has been reported to form Al-substituted C–S–H phases (Barzgar et al., 2020; L'Hopital et al., 2015). Due to the similar charge-to-size ratio (z/d) and aqueous speciation in hyperalkaline systems, aluminum has been proposed as possible chemical analogue to assess the uptake of beryllium by cementitious materials (Ochs et al., 2016).

Molecular modelling allows interpretation of the experimentally observed interfacial behaviour on the atomic and molecular scale considering the effects of the structure and composition of the surface on the interaction. C–S–H interfaces are complex systems with disordered structures (Grangeon et al., 2017; Monteiro et al., 2019), and larger system sizes and longer simulation times, compared to routine quantum simulation set-ups, are therefore required to obtain meaningful statistical data to describe sorption processes (Mutisya et al., 2017). Quantum chemical calculations are more precise, but they are computationally very expensive, and thus mostly used either to describe preselected sorption sites on the surface, and incorporated species, where ion mobility is less important (Kremleva et al., 2020; Lange et al., 2018), or to study substitution reactions with simpler and smaller systems (Churakov et al., 2017). When sorption sites are not known, molecular dynamics (MD) simulations are typically used to study sorption mechanisms of ions on cementitious materials (Androniuk et al., 2020; Bu et al., 2019; Honorio et al., 2019), and this method was chosen to study the sorption of beryllium on the C–S–H surface.

Many computational studies have been previously conducted to describe the behaviour of beryllium complexes in aqueous solutions on a molecular scale, and significant efforts have been dedicated to go beyond the classical two-body potentials for aqueous Be^{2+} ions to describe its interactions realistically using molecular dynamics (Azam et al., 2009; D'Incal et al., 2006; Gnanakaran et al., 2008; Raymond et al., 2020). The 12-6-4 Lennard-Jones-type nonbonded parameters for Be^{2+} and Ca^{2+} have been used in our simulations. This model can reproduce the correct geometry for the binding of cations as observed in crystal structures, and the experimental hydration free energies (De et al., 2020; Li et al., 2014; Li et al., 2020). Combinational analysis of the time-averaged local structures and 1D and 2D density profiles for target aqueous species together with the experimental data provides an insight into the prevailing uptake mechanisms and the preferential sorption sites on the surface.

In the context of the EU funded collaborative project ‘‘Cement-based materials, properties, evolution, barrier functions’’ (Cebama), the present study aims at a comprehensive investigation of beryllium uptake by cementitious systems. The cement materials investigated include an ordinary Portland cement in the degradation stage II, a low pH cement defined as the Cebama reference cement (Vehmas et al., 2020), as well as C–S–H phases with Ca:Si 0.6, 1.0 and 1.6. The latter phases are expectedly the main sink of Be(II) in cement. Sorption experiments with TiO_2 are performed to gain additional insight on the mechanisms driving the uptake of Be(II) in hyperalkaline systems. Surface complexation is known to be the main uptake mechanism in TiO_2 systems (Bouby et al., 2010; Tits et al., 2014; Tits et al., 2011; Tits et al., 2015), thus allowing to distinguish the possible incorporation mechanism into the C–S–H phases. Beyond the quantitative investigation of the uptake on the basis of sorption kinetics, sorption isotherms and distribution ratios, the use of molecular dynamics provides a very accurate description of the surface processes driving the uptake of beryllium at molecular scale. This work complements and further extends our previous study on the solubility, hydrolysis and thermodynamic description of Be(II) in alkaline to hyperalkaline conditions relevant for cementitious systems (Çevirim-Papaioannou et al., 2020).

2. Experimental

2.1. Chemicals and analytical methods

All solutions and samples were prepared with purified water (Milli-Q academic, Millipore, 18.2 MΩ cm) purged with Ar for at least 1 h before use to remove CO₂(g) dissolved in solution. Sample preparation, handling and equilibration were performed in an Ar-glove box (O₂ < 1 ppm) at T (22 ± 2) °C. BeSO₄·4H₂O (99.99%), NaCl EMSURE, KCl EMSURE, NaOH Titrisol, KOH Titrisol and HCl Titrisol were obtained from Merck. CaO, Na₂SO₄, Na₂O₇Si₃, CaCl₂·H₂O, CaCO₃, Ca(OH)₂ and H₂SO₄ (96%) were all of analytical grade and were purchased from Merck. TiO₂ (Degussa P-25) and SiO₂ (AEROSIL 300) were obtained from Evonik Industries.

The pH in solution was measured using combination pH electrodes (ROSS Orion, with 3.0 M KCl as filling solution). Calibration of the electrode was performed with standard pH buffers (pH 1–12, Merck).

2.2. Sorption materials used in this study

A monolith of a hydrated cement paste (HCP, CEM I 42,5 N BV/SR/LA type) was provided by the Swedish Nuclear Fuel and Waste Management Company (SKB) in Sweden. The HCP was milled, sieved to a particle size of <100 μm as described in Tasi et al. (2021) and stored under Ar atmosphere until use in the sorption experiments. An extensive characterization of the HCP (XRD, TGA-DSC, XPS, BET) is provided in Tasi et al. (2021). The surface area of the powder material used in the present study was determined by Tasi and co-workers as 79.2 m²·g⁻¹.

A monolith of the CEBAMA reference cement (low pH cement, CEM I 42,5 MH/SR/LA mixture with silica fume, BFS and plasticiser pantarhit) was provided by the Technical Research Centre of Finland (VTT) (Vasconcelos et al., 2020; Vehmas et al., 2020) within the CEBAMA project. All surfaces (≈ 5 mm thickness) of the cement monolith were cut under Ar atmosphere using a radial saw in order to remove the potentially carbonated surface. Afterwards, the cement block was crushed and powdered with a grinder, then sieved to a particle size of < 63 μm and stored under Ar atmosphere. The characterization of the CEBAMA reference cement is reported in Vasconcelos et al. (2020). The latter authors reported a Ca:Si (0.9 ± 0.1) for the hydrated material after a curing time of 18 months.

Boiled and degassed ultrapure water was used in the synthesis of C–S–H phases. All C–S–H phases were prepared by mixing Ca(OH)₂-Prolabo which was heated at 1000 °C for 24 h and SiO₂ (Aerosil 200, Degussa) in inert atmosphere (N₂ glovebox). C–S–H phases with Ca:Si ratio ranging from 0.6 to 1.6 were precipitated at 22 °C. Further details on the preparation and characterization of C–S–H phases are reported elsewhere (Gaboreau et al., 2020).

The commercial TiO₂ used in this work was extensively characterized by XRD, BET, photon correlation spectroscopy and FTIR in a previous study (Bouby et al., 2010). The authors reported a composition of 85% anatase and 15% rutile, with an average surface area of 50.6 m²

g⁻¹. Bouby and co-workers determined also the point of zero charge (pzc) of this material as pH_{pzc} = 6.1. TiO₂ is a sparingly soluble metal oxide (Schmidt et al., 2009), which has been extensively used in previous sorption studies covering acidic to hyperalkaline pH conditions (Bouby et al., 2010; Tits et al., 2014; Tits et al., 2011; Tits et al., 2015). TiO₂ is considered in this work as a reference material to assess the surface complexation behavior of Be(II) within the investigated pore water conditions.

2.3. Preparation of cement pore waters

Sorption experiments with HCP targeted the degradation stage II of cement. To obtain the corresponding pore water solution, the powdered HCP (≤ 100 μm) was immersed in 1 L of Milli-Q water at a solid to liquid ratio (S:L) of 25 g·L⁻¹. This suspension was shaken regularly for two weeks under Ar atmosphere. Thereafter, the supernatant was removed and eventually, the same volume of Milli-Q water was contacted with the HCP to retain the same S:L ratio. The resulting pore water is representative of the cement degradation stage II, i.e. low alkali content, pH ≈ 12.5 and [Ca]_{tot} ≈ 2·10⁻² M as buffered by portlandite.

The artificial pore water of the CEBAMA reference cement was prepared as described in Ait Mouheb et al. (2019). Corresponding amounts of KOH, CaO, Na₂SO₄, Na₂O₇Si₃, CaCl₂·H₂O, CaCO₃ and Ca(OH)₂ were dissolved in 660 mL of Milli-Q water, and the pH adjusted with a 0.04 M H₂SO₄ solution. The resulting pore water was filtered with membrane filter (0.2 μm, Millipore) before the preparation of the sorption samples.

Artificial pore water for C–S–H phases with Ca:Si = 0.6, 1.0 and 1.6 were prepared with Milli-Q water, CaO and SiO₂ targeting the pH, [Ca] and [Si] of the original C–S–H phases as reported in (Gaboreau et al., 2020).

Besides the investigated cementitious systems, the uptake of Be(II) by TiO₂ was studied in contact with the pore water solutions of C–S–H 1.0, C–S–H 1.6 and HCP in the degradation stage I. The latter system was considered to provide an upper pH limit in the sorption experiments with TiO₂. The corresponding artificial pore water was prepared as described in Çevirim-Papaioannou et al. (2021), and is characterized by pH values of ≈ 13.2, [Na] = 0.032 M, [K] = 0.075 M, [Ca] = 4.1·10⁻⁴ M and [Si] = 1.1·10⁻⁴ M.

2.4. Sorption experiments

All experiments were carried out under Ar atmosphere. The sorption samples with cement (HCP or low pH), C–S–H phases or TiO₂ were prepared with 20 mL of the corresponding pore water solution (see section 2.4) and a S:L = 0.2 or 2 g·L⁻¹. BeSO₄ stock solutions (0.35–10⁻³ M) were used to obtain the targeted initial Be concentrations, i.e. 3·10⁻³ M ≤ [Be]₀ ≤ 10⁻⁶ M. The range of Be concentration considered for each system was selected on the basis of the solubility data reported in Çevirim-Papaioannou et al. (2020) for α-Be(OH)₂. Table 1 summarizes the experimental boundary conditions considered for the sorption experiments.

Table 1

Experimental conditions considered in the uptake experiments with Be(II), cementitious materials and TiO₂. p.w. refers to the cementitious pore waters used in the experiments with TiO₂.

Sorbent		S/L [g·L ⁻¹]	Eq. time (d)	pH	Initial [Be] [M]	Number of samples
C–S–H phases	Ca:Si 0.6	0.2, 2	4–145	10.1	3·10 ⁻⁶ –1·10 ⁻³	12
	Ca:Si 1.0	2		12.1	1·10 ⁻⁶ –3·10 ⁻³	8
	Ca:Si 1.6	2		12.6	1·10 ⁻⁶ –2·10 ⁻³	7
HCP, deg. stage II		2	4–145	12.7	1·10 ⁻⁶ –3·10 ⁻³	7
Low pH cement (CEBAMA ref. cement)		2	60	11.4	1·10 ⁻⁶ –3·10 ⁻³	7
TiO ₂	p.w. C–S–H 1.0	2	1–20	12.1	1·10 ⁻⁵ –3·10 ⁻⁴	4
	p.w. C–S–H 1.6	2		12.6	1·10 ⁻⁵ –3·10 ⁻⁴	4
	p.w. HCP deg. stage I	2		13.2	1·10 ⁻⁵ –3·10 ⁻⁴	4

Sorption samples with HCP (deg. stage II) and low pH cement were contacted with the corresponding pore water solutions. Stock suspensions (S:L 4 g L⁻¹) of C–S–H phases with Ca:Si 0.6, 1.0 and 1.6 were diluted with the artificial pore waters of each phase in order to obtain the targeted S:L 2 g L⁻¹. Due to the strong uptake observed for this system, additional samples with S:L 0.2 g L⁻¹ were prepared for C–S–H 0.6. The samples containing TiO₂ were prepared by contacting the solid material with pore waters of C–S–H 1.0 (pH 12.1), C–S–H 1.6 (pH 12.6) and HCP (degradation stage I, pH 13.2), in all cases with S:L 2 g L⁻¹.

Beryllium concentration and pH in each sample were monitored at regular time intervals from 1 to 145 days until equilibrium conditions were attained. An aliquot of the supernatant (200–500 µL) of each sample was centrifuged for 2–3 min with 10 kD filters (2–3 nm cut-off Nanosep® centrifuge tubes, Pall Life Sciences) to separate colloids or suspended particles. After centrifugation, the respective volume of the filtrate was diluted (1:40 to 1:1000, depending upon initial Be concentration) in 2% ultrapure HNO₃, and [Be] was quantified by ICP–MS (inductively coupled plasma mass spectrometry, Perkin Elmer ELAN 6100). The accuracy of ICP–MS measurements was ± 2–5%. Detection limit varied between 10^{-5.5} and 10⁻⁸ M depending on the dilution factor. Previous tests experiments confirmed that the sorption of Be(II) in the 10 kD filters is not significant in the pH- and [Be]-range investigated in this study.

Before the addition of beryllium in each sample as well as after attaining the thermodynamic equilibrium in all investigated systems, the concentrations of Ca, K and Na were quantified using ICP–OES (inductively coupled plasma–optical emission spectroscopy, Perkin–Elmer 4300 DV) in order to determine the composition of the aqueous phase. The replicate aliquots taken from the supernatant (200–500 µL) were ultrafiltrated (2–3 min centrifugation with 10 kD filters) and diluted (1:40 to 1:100) in 2% HNO₃. The detection limit of this technique is ≈ 10⁻⁴ to ≈ 10⁻⁵ M, depending on the measured element and dilution factor.

Sorption kinetics were investigated following the evolution of the distribution ratio, R_d (in L kg⁻¹), as a function of time. R_d values were calculated as the ratio of beryllium concentration in the solid ($[Be]_{solid}$, in mol kg⁻¹) and aqueous ($[Be]_{aq}$, in M) phases:

$$R_d = \frac{[Be]_{sol} \cdot V}{[Be]_{aq} \cdot m} = \frac{[Be]_0 \cdot [Be]_{aq} \cdot V}{[Be]_{aq} \cdot m} \quad (1)$$

where $[Be]_0$ is the initial beryllium concentration, V is the volume of sample (L) and m is the mass of the solid used as sorbent (kg).

The uptake of beryllium under equilibrium conditions i.e. after contact time of > 125 days for cementitious phases was evaluated in terms of sorption isotherms (log $[Be]_{solid}$ vs. log $[Be]_{aq}$), although distribution ratios were also used to compare the uptake of Be(II) with other metal ions.

2.5. Computational methods

Molecular dynamics was used to study the sorption of beryllium on the C–S–H surface. Calculations were performed using the (001) surface of C–S–H (Fig. 1). This is the most typical cleavage plane of C–S–H, parallel to silicate chains and CaO-layers, where the least number of bonds had to be broken. The model of this surface was taken from (Jamil et al., 2020). All the bridging Si were removed to get the structure of C–S–H with Ca:Si > 1.4 following available experimental spectroscopy data (Cong et al., 1996; Roosz et al., 2018). The silanol groups were deprotonated, and missing Si were replaced by Ca²⁺. The deprotonated oxygen atoms of the surface were assigned a partial charge of q_{onb}

1.3|e|, higher than the protonated ones in the standard ClayFF model (Androniuk et al., 2017; Kirkpatrick et al., 2005a; Kirkpatrick et al., 2005b).

The interfacial aqueous solution contained 6 ions of Be(OH)₃⁻, and 4 Be(OH)₄²⁻ with ~5400 H₂O molecules, which approximately corresponds to 0.1 M beryllium ion concentration and pH of ~12.7, as estimated using thermodynamic data reported in Çevirim-Papaioannou et al. (2020). This relatively high concentration had to be used in the simulations for better statistical sampling. The possible formation of polynuclear Be-species under these conditions was also evaluated in the calculations. Aqueous hydroxyl ions were added to the system in order to maintain the total electrostatic neutrality of the models. The calculation routine details can be found in the Supplementary Data (SD2.5).

The interatomic interaction parameters for C–S–H and H₂O were taken from the ClayFF (Cygan et al., 2004), and its later modifications for cement systems (Kalinichev et al., 2007; Kirkpatrick et al., 2005;

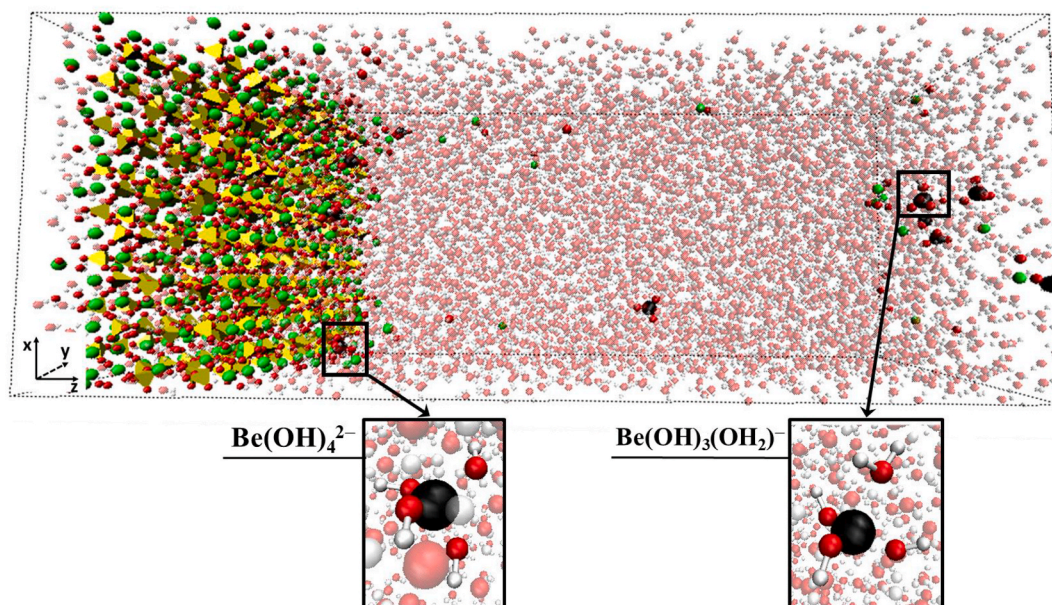


Fig. 1. Snapshot of (001) C–S–H simulation supercell. Colour scheme: Si – yellow; Ca – green; O – red; H – white; Be – black. Water molecules shown in transparent for clarity. (For interpretation of the references to colour in this figure legend, the reader is referred to the Web version of this article.)

Mishra et al., 2017). The 12-6-4 Lennard-Jones type non-bonded parameters for Ca^{2+} and Be^{2+} , which include the contribution from the ion-induced dipole interaction, were taken from Li and Merz (Li and Merz, 2014).

3. Results and discussion

3.1. Characterization of the pore water solutions in equilibrium with cement and C–S–H phases

Table SD-1 in the Supplementary Data summarizes the pore water composition (pH and concentrations of Na, K, Ca and Si) in contact with the investigated cement systems (C–S–H phases with Ca:Si 0.6, 1.0 and 1.6, HCP in degradation stage II and low pH cement). These values are in line with data available in the literature for analogous systems (Ait-Mouheb, 2021; Atkins et al., 1992; Gaboreau et al., 2020; Pointeau et al., 2004; Tasi, 2018; J. Tits, Wieland, et al., 2006). As expected, C–S–H phases are characterized by an increase of pH and Ca concentration with increasing Ca:Si ratio. Similar pH and [Ca] are determined for C–S–H 1.6 and HCP in the degradation stage II, thus reflecting the predominance of C–S–H phases with high Ca:Si ratio in this degradation stage of cement. The values of pH and [Ca] in both systems are consistent with an equilibrium with portlandite.

Porewater compositions were also characterized after completing the sorption experiments with Be(II). Table SD-2 in the Supplementary Data shows that no significant changes in the composition of the pore water occurred within the uptake process, except for the low pH cement equilibrated with the highest initial beryllium concentration ($[\text{Be}]_0$ $3.0 \cdot 10^{-3}$ M), for which a decrease of ≈ 0.3 pH-units was observed. These results support that the sorption process did not alter the composition of the sorbent material.

3.2. Sorption kinetics

Fig. 2 shows the sorption kinetics (as $\log R_d$ vs. time) for the uptake of Be(II) by C–S–H 1.6, HCP and TiO_2 . A similar uptake behavior is observed for C–S–H 1.6 and HCP, thus highlighting the known analogies between these systems. In both cases, a fast sorption taking place within 4 days ($\log R_d \approx 4.5$) is followed by a slower increase of the $\log R_d$ up to ≈ 5.5 , with equilibrium conditions being attained at $t \geq 60$ days. This step-wise behavior expectedly reflects the involvement of two uptake mechanisms, possibly corresponding to a fast surface complexation

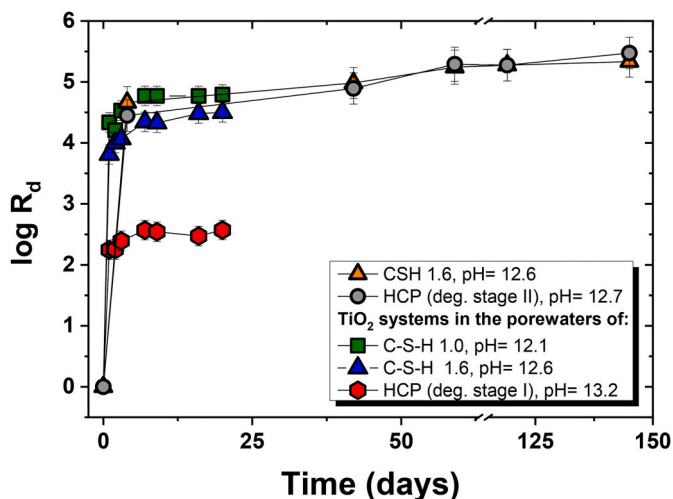


Fig. 2. Kinetics of the Be(II) uptake by C–S–H 1.6, HCP (degradation stage II) and TiO_2 (pore water solutions of C–S–H 1.0, 1.6 and HCP degradation stage I). Initial Be(II) concentrations are 10^{-4} M (C–S–H and HCP) and 10^{-4} M (TiO_2). R_d values expressed in $\text{L} \cdot \text{kg}^{-1}$.

process followed by the slower incorporation of Be(II) into the structure of C–S–H. A similar behavior has been previously described for other strongly sorbing metal ions, e.g. Zn(II), Nd(III), Eu(III), Np(IV) or U(VI) (Gaona et al., 2011; Mandaliev et al., 2010a; Mandaliev et al., 2010b; Pointeau et al., 2004; Pointeau et al., 2001; Schlegel et al., 2004; Stumpf et al., 2004; Tits et al., 2011; Tits et al., 2015; Ziegler et al., 2001).

A much faster equilibrium ($t \geq 7$ days) is attained in the three investigated TiO_2 systems where no incorporation process is possible. TiO_2 is often considered as a model compound for the study of adsorption processes (Bouby et al., 2010; Guo et al., 2005; Hakem et al., 1996; Tits et al., 2014; Tits et al., 2015; Tits and Wieland, 2018), and thus the fast uptake observed for Be(II) is exclusively attributed to surface complexation. Although showing similar uptake kinetics, significant differences arise for the adsorption of Be(II) onto TiO_2 at pH 12.1 ($\log R_d \approx 4.8$), 12.6 ($\log R_d \approx 4.5$) and 13.2 ($\log R_d \approx 2.5$). An extensive discussion of this observation is provided in Sections 3.4 and 3.5.

3.3. Uptake of Be(II) by C–S–H, HCP (deg. stage II) and “low pH” cement: sorption isotherms

Sorption isotherms of Be(II) (as $\log [\text{Be}]_{\text{solid}}$ vs. $\log [\text{Be}]_{\text{aq}}$) for the uptake by C–S–H 1.0, C–S–H 1.6 and HCP (deg. stage II) are shown in Fig. 3. The experimental window in systems C–S–H 0.6 and low pH cement is limited by the low solubility of $\alpha\text{-Be}(\text{OH})_2(\text{cr})$ at these pH values ($\approx 10^{-7}$ to $\approx 10^{-6}$ M, see Çevirim-Papaioannou et al., 2020) and the detection limit of the ICP-MS technique ($\approx 10^{-8}$ M). For this reason, insufficient data for the construction of the sorption isotherms were collected for these systems, and only $\log R_d$ values calculated on the basis of experiments with the lowest $[\text{Be}]_0$ are discussed in Section 3.5.

Fig. 3 shows consistent Be(II) sorption data for systems C–S–H 1.0, C–S–H 1.6 and HCP. All sorption isotherms show a linear trend over three orders of magnitude in $[\text{Be}]_{\text{aq}}$, in all cases with a slope of ≈ 1 . This observation suggests that the same mechanism is controlling the uptake of beryllium under the investigated conditions. The grey regions in the figure illustrate the solubility limits of $\alpha\text{-Be}(\text{OH})_2(\text{cr})$ calculated at pH 12.1 (light grey, C–S–H 1.0) and 12.6 (dark grey, C–S–H 1.6 and HCP) (Çevirim-Papaioannou et al., 2020). These regions define lower solubility limits of Be(II) in the investigated conditions, bearing in mind that the formation of amorphous $\text{Be}(\text{OH})_2(\text{am})$ expected in early

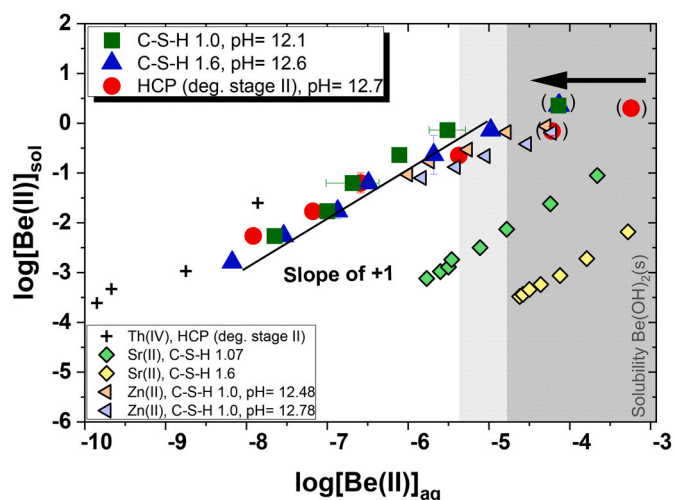


Fig. 3. Sorption isotherms of Be(II) taken up by C–S–H 1.0, 1.6 and HCP (deg. stage II). Grey regions correspond to the solubility limits of $\alpha\text{-Be}(\text{OH})_2(\text{cr})$ calculated at pH = 12.1 (light grey, C–S–H 1.0) and 12.6 (dark grey, C–S–H 1.6 and HCP) using thermodynamic data reported in Çevirim-Papaioannou et al. (2020). Sorption isotherms of Zn(II) (C–S–H 1.0 at pH = 12.48 and 12.78, Ziegler et al., 2001), Sr(II) (C–S–H 1.0 and 1.6, Tits et al., 2006a,b) and Th(IV) (HCP deg. stage II, Tits and Wieland, 2018) are appended for comparison.

precipitation stages may result in solubility limits 1–2 orders of magnitude higher. A slow decrease in the concentration of Be(II) is observed for the three samples in the dark grey region in Fig. 3, corresponding to sorption experiments with $[Be]_0$ $10^{-2.5}$ and 10^{-3} M. These samples are considered to be controlled by solubility, with the slow decrease in concentration with time reflecting the transformation of the amorphous $Be(OH)_2(am)$ into α - $Be(OH)_2(cr)$ as reported in Çevirim-Papaioannou et al. (2020).

Fig. 3 shows also the sorption isotherms previously reported for the uptake of Sr(II) (C–S–H 1.07 and 1.6; Tits et al., 2006b), Zn(II) (C–S–H 1.0; Ziegler et al., 2001a,b) and Th(IV) (HCP deg. stages I and II; Tits and Wieland, 2018). In spite of belonging to the same group in the periodic table, Sr(II) shows a much weaker and pH-dependent uptake compared to the Be(II) data obtained in the present study. These observations suggest that a different mechanism is controlling the uptake of both alkali-earth metals. Among all divalent ions, sorption isotherms reported for the uptake of Zn(II) by C–S–H (Ziegler et al., 2001) show the closest behavior to the sorption data determined in the present study for Be(II). Although Ziegler and co-workers observed the precipitation of $CaZn_2(OH)_6 \cdot 2H_2O(s)$ above $\log [Zn(II)] \approx 4.2$, the agreement with Be(II) sorption data is excellent down to $[Zn(II)] \approx 6$. For the sake of comparison, Fig. 3 includes also the sorption isotherms reported for a strongly sorbing metal, i.e. Th(IV). Tits and Wieland reported the sorption isotherms for the uptake of Th(IV) by HCP (deg. stages I and II) (Tits and Wieland, 2018). The authors targeted very low metal concentrations (10^{-14} – 10^{-7} M, using ^{228}Th) to avoid the precipitation of the sparingly soluble $ThO_2(am, hyd)$. In spite of covering largely different metal concentrations, the overall uptake and the trend with increasing pH reported for Th(IV) by Tits and Wieland (2018) are similar to the results obtained in this study for Be(II). An extensive discussion on the uptake of Be(II) by C–S–H phases and cement in terms of $\log R_d$ values, as compared to other metal cations is provided in Section 3.5.

3.4. Uptake of Be(II) by TiO_2 : sorption isotherms

Fig. 4 shows the sorption isotherms for the uptake of Be(II) by TiO_2 in equilibrium with pore water solutions of C–S–H 1.0, C–S–H 1.6 and HCP (deg. stage I). In all cases, a linear sorption with slope $\approx +1$ is observed. In contrast to C–S–H phases and HCP, the uptake of Be(II) by TiO_2 is strongly affected by pH, with a significant drop in $\log [Be]_{solid}$ observed

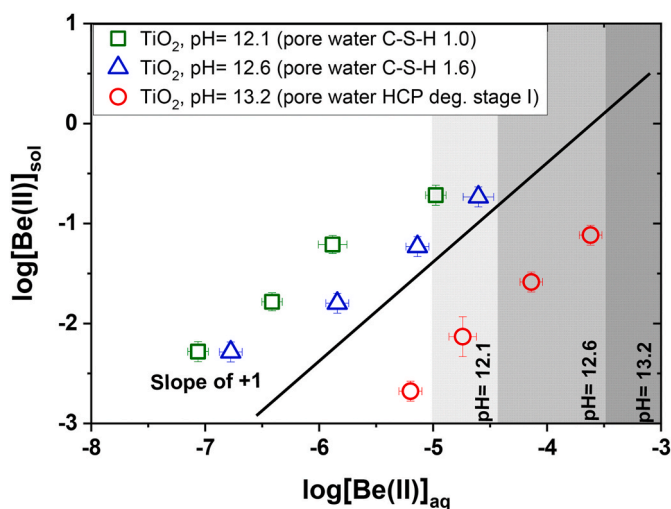


Fig. 4. Be Sorption isotherms of Be(II) taken up by TiO_2 equilibrated with pore water solutions of C–S–H 1.0, 1.6 and HCP (deg. stage I). Grey regions correspond to the solubility limits of α - $Be(OH)_2(cr)$ calculated at pH = 12.1 (light grey, C–S–H 1.0), 12.6 (dark grey, C–S–H 1.6) and 13.2 (dashed grey, HCP deg. stage I) using thermodynamic data reported in Çevirim-Papaioannou et al. (2020).

between pH 12.1 and 13.2. These large differences can be partly explained by the different aqueous speciation of Be(II) at these pH values, with the predominance of $Be(OH)_3^-$ and $Be(OH)_4^{2-}$ at pH 12.1 and 13.2, respectively, and assuming that the latter species does not sorb onto TiO_2 . Based on the concept of electrostatic inter-ligand repulsion proposed by Neck et al. (2001) and the definition of limiting hydrolysis species for metal ions, Tits and co-workers elaborated on the uptake of highly hydrolyzed metal ions by TiO_2 in hyperalkaline pH conditions ($10 \leq pH \leq 14$) (Tits et al., 2014). This approach was successfully applied to quantitatively explain the decrease in $\log R_d$ values induced by the predominance of the limiting hydrolysis complexes $Np(V)O_2(OH)_2^-$ and $Np(VI)O_2(OH)_4^{2-}$ in the aqueous phase (with n hydroxo-groups), which accordingly hindered the step-wise formation of surface complexes with (n + 1) hydroxo-/oxo-groups. A similar effect could be claimed to explain the decreased uptake of Be(II) by TiO_2 in the pH-range where the limiting complex $Be(OH)_4^{2-}$ prevails.

The presence of Ca in hyperalkaline solutions has been reported to compensate the negative charge of the TiO_2 surface, and thus enhance the adsorption of negatively charged aqueous species (Tits et al., 2014). From the three investigated TiO_2 systems, the one in equilibrium with the pore water of HCP in the degradation stage I is characterized by the lowest Ca concentration ($7.5 \cdot 10^{-5}$ M), which possibly contributes to the weaker sorption observed for this system. The combination of both factors (pH and [Ca]) is considered to drive the large differences in the uptake of Be(II) by TiO_2 systems.

3.5. Discussion of $\log R_d$ values and comparison with other M(II)

Fig. 5a summarizes the $\log R_d$ values of all investigated C–S–H, cement and TiO_2 systems. The figure includes also the $\log R_d$ value for the uptake of Be(II) by HCP in the degradation stage I as reported in Çevirim-Papaioannou et al. (2021). Dashed lines in the figure represent the highest distribution ratios ($\log R_{d,max}$) that can be quantified for experiments at S/L 0.2 and $2 g L^{-1}$, considering a detection limit of $\approx 10^{-8}$ M. Very high $\log R_d$ values (5–7, with R_d in $L kg^{-1}$) are determined for all C–S–H and cement materials investigated. The strongest sorption ($\log R_d \approx 7$) is observed for the system C–S–H 0.6, which is characterized by the lowest pH conditions investigated in this study (pH ≈ 10). The uptake decreases to $\log R_d \approx 6.1$ for low pH cement (pH ≈ 11.5), and further to $\log R_d \approx 5$ for C–S–H 1.0 (pH ≈ 12.1). Above this pH, all investigated cement systems hold similar distribution ratios, with $\log R_d \approx 5$. We hypothesize that the predominance of the neutral aqueous species $Be(OH)_2(aq)$ in the pore water of C–S–H 0.6 may be responsible for the stronger uptake observed for this system.

The $\log R_d$ values determined in this work for Be(II) are significantly higher than those reported for the uptake of other divalent cations by C–S–H and HCP, i.e. Sr(II) ($1 \leq \log R_d \leq 3.3$), Ba(II) ($1.3 \leq \log R_d \leq 3.7$), Ra(II) ($2 \leq \log R_d \leq 4.1$), Fe(II) ($\log R_d \approx 2$) or Pb(II) ($2.9 \leq \log R_d \leq 3.8$), with the exception of Zn(II) ($4.3 \leq \log R_d \leq 5.5$) (Mancini et al., 2020; Missana et al., 2017; Olmeda et al., 2019; Pointeau et al., 2001; Tits et al., 2006a, b; Wieland, 2014; Wieland et al., 2008; Wieland and Van Loon, 2003; Ziegler et al., 2001a).

The large differences between $\log R_d$ values of M(II) possibly reflect the different mechanisms controlling the uptake of these metal cations by cementitious materials. The uptake of alkali-earth metals by C–S–H phases is driven by ion-exchange in the case of Sr(II) (Tits et al., 2006b), but is controlled by a combination of surface complexation and ion-exchange in the case of Ba(II) and Ra(II) (Missana et al., 2017; Olmeda et al., 2019; Tits et al., 2006a). Bernard and co-workers found no evidence for the uptake of Mg(II) by C–S–H phases, and instead reported the co-existence of two separate phases (C–S–H and M–S–H) within $10 \leq pH \leq 11$ (Bernard et al., 2018a; Bernard et al., 2018b).

Fe(II), Pb(II) and Zn(II) are characterized by the formation of anionic hydrolysis species in alkaline to hyperalkaline pH conditions. The solution chemistry of Fe(II) and Pb(II) is dominated by the species $M(OH)_3^-$ above pH ≈ 11 –12 (Bruno et al., 2018; Walsh, 2009). Based on their XRD

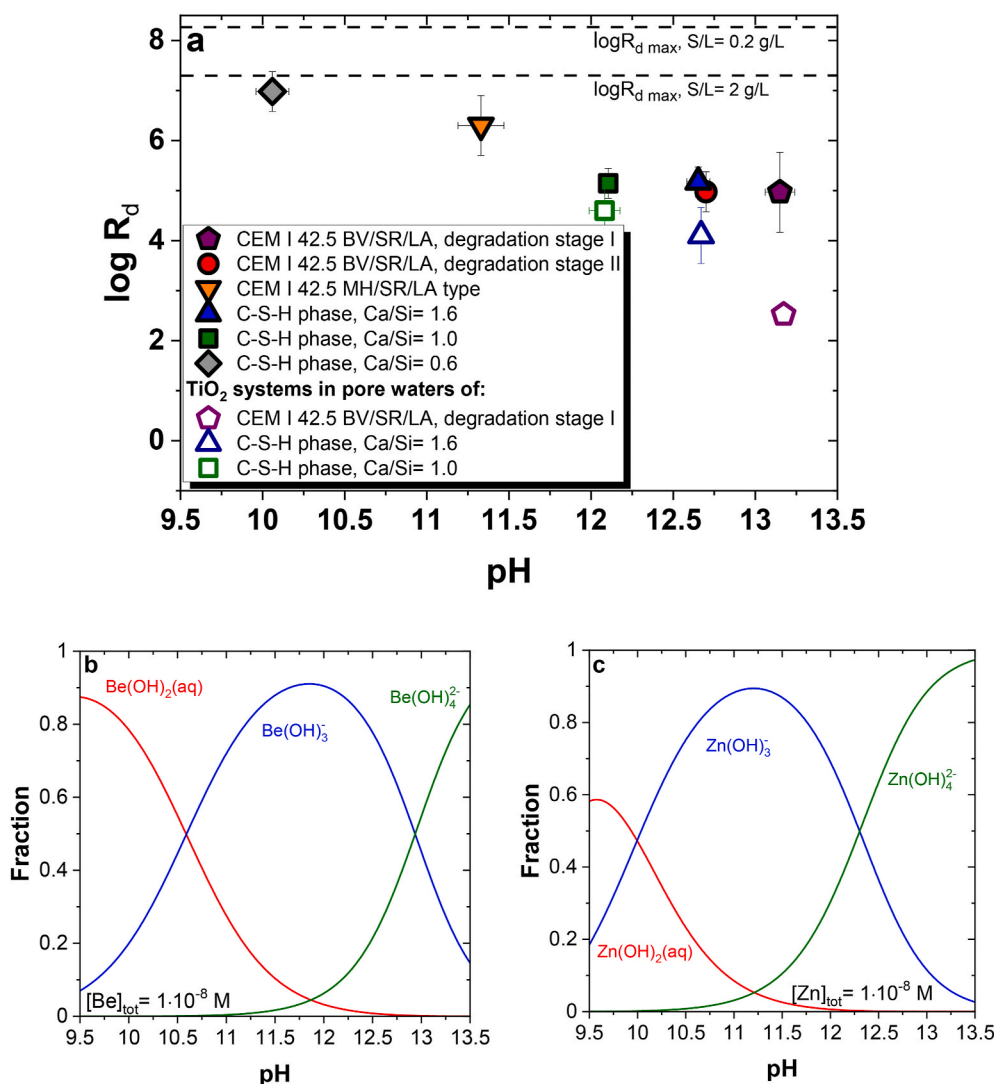


Fig. 5. (a) $\log R_d$ values determined in this work for the uptake of Be(II) by C-S-H (0.6, 1.0 and 1.6), HCP (deg. stage II), “low pH” cement and TiO₂. $\log R_d$ values reported in Çevirim-Papaioannou et al. (2021) for the uptake of Be(II) by HCP (deg. stage I) are appended for comparison. (b) Fraction diagrams of Be(II) and (c) Zn(II) calculated for $[M(II)]_{\text{tot}} = 1 \cdot 10^{-8}$ M and $9.5 \leq \text{pH} \leq 13.5$ using thermodynamic data reported in Çevirim-Papaioannou et al. (2020) and Brown and Ekberg (2016), respectively.

and EXAFS observations, Mancini and co-workers reported the presence of both surface- and interlayer-bound Fe(II) species in the sorption experiments with C-S-H phases (Mancini et al., 2020). In line with these observations, Pointeau et al. proposed surface complexation as main mechanism for the uptake of Pb(II) by C-S-H (Pointeau et al., 2001a, b).

In spite of their largely different ionic radii ($r_{Zn^{2+}} = 0.06$ nm; $r_{Be^{2+}} = 0.027$ nm; values corresponding to a CN = 4; Shannon, 1976), Zn(II) and Be(II) are characterized by a strong hydrolysis and the predominance of $M(OH)_3$ and $M(OH)_4^{2-}$ in hyperalkaline pH conditions (see Fig. 5b and c). Zn(II) shows the strongest uptake by C-S-H of all previously reported divalent cations, with $\log R_d$ values slightly lower but comparable to Be(II). Based on their kinetic and spectroscopic (XAFS) data, Ziegler and co-workers reported a step-wise uptake of Zn(II) with a fast ($t \leq 4$ days) surface complexation process followed by the slower ($t \leq 87$ days) incorporation in the C-S-H interlayer (Ziegler et al., 2001a, 2001b). The similar kinetic behavior observed in this work for Be(II) possibly hints to analogous uptake mechanisms for both metal ions.

The values of $\log R_d$ determined in this work for Be(II) are also in line with data reported for strongly sorbing metal ions such as lanthanides or actinides in the +III and +IV oxidation states (Haussler et al., 2018; Pointeau et al., 2004; Tasi, 2018; Tits and Wieland, 2018; Wieland, 2014; Wieland and Van Loon, 2003). The pH-independent behavior observed for the uptake of these elements by C-S-H and HCP can be partially explained by the invariant aqueous speciation within the pH-region covered by the different degradation stages of cement, i.e. Ln

(III)/An(III)(OH)₃(aq) and An(IV)(OH)₄(aq). For the Ln(III)/An(III) systems, several spectroscopic studies (TRLFS, EXAFS) support their incorporation in the CaO-layer of C-S-H, which can be rationalized by the similar ionic radii of Ln^{3+}/An^{3+} and Ca^{2+} . In the case of An(IV), EXAFS studies hint to their incorporation in the interlayer of C-S-H (Gaona et al., 2011; Haussler et al., 2018).

The comparison of the uptake of Be(II) by C-S-H/HCP and TiO₂ in absolute terms is not straightforward due to the differences in the surface area of these materials (see Section 2.2). However, differences in the uptake trends observed for C-S-H/HCP and TiO₂ can be considered to gain indirect evidence on the mechanism controlling the uptake of Be(II) in cementitious systems. A significant decrease in the uptake is observed for TiO₂ systems between pH = 12.1 ($\log R_d \approx 4.7$) and 13.2 ($\log R_d \approx 2.5$). As discussed in Section 3.4, this trend is partly explained by the increasing fraction of the limiting complex $Be(OH)_4^{2-}$ in solution, which prevents the step-wise formation of the surface complex $>S-O-Be(OH)_4$. Within the same pH-region and boundary conditions, the uptake of Be(II) by C-S-H and HCP remains nearly constant at $\log R_d \approx 5$. Together with the step-wise kinetic behavior, this observation is taken as indirect evidence for the incorporation of Be(II) in the C-S-H structure, as opposed to the surface complexation mechanism reported to control the uptake of metal ions by TiO₂ (Bouby et al., 2010; Tits et al., 2011; Tits et al., 2014, among others).

Wieland and Van Loon attempted to rationalize the uptake of metal ions by cement using the charge-to-size relationship (z/d) of the metal

ion, where z is the charge of the metal ion and d is the M–O interatomic distance, with $d = r_{M^{z+}} + r_{O^{2-}}$. This relationship gives insight on the polarising effect of cations on anionic counter-ions (Wieland and Van Loon, 2003). As highlighted by these authors, this approach explains the uptake on the basis of the ionic character of the bonding and irrespective of the underlying uptake mechanism, thus largely oversimplifying the uptake process. However, the approach appears useful to qualitatively explain the general trends observed for the uptake of metal ions by HCP, connecting the very strong sorption observed in this work for Be(II) with the uptake of apparently very different elements such as lanthanides or actinides. The original figure reported by Wieland and Van Loon for the uptake of Cs(I), Sr(II), Eu(III), Th(IV) and Sn(IV) by HCP (deg. stage I) has been extended in this work to Be(II) and other metal ions, including as well data for the uptake of these metals by HCP in the degradation stage II.

Fig. 6 shows two clear trends in the uptake of metal ions by HCP (deg. stages I and II). Lower $\log R_d$ values are obtained for metal ions with $z/d < 1$, which show also a clear tendency to decreasing $\log R_d$ with decreasing z/d . The uptake of these metals ions by cement and C–S–H phases has been predominantly reported as ion-exchange and/or surface complexation. Higher and nearly constant $\log R_d$ values ($\log R_d \approx 5 \pm 1$) are reported for those metal ions with $z/d \geq 1$. Spectroscopic evidences have systematically hinted to the incorporation in the C–S–H structure (i.e. CaO-layer or interlayer) as main uptake mechanism for the metal ions in this z/d region. We note the excellent agreement in the $\log R_d$ values determined in this work or reported in Çevirim-Papaioannou et al. (2021) for Be(II) ($z/d = 1.20$), with data reported for Eu(III) ($z/d = 1.13$) or Am(III) ($z/d = 1.20$). This exercise gives confidence in the incorporation of beryllium to the group of strongly sorbing metal ions in cementitious systems, usually restricted to lanthanides, actinides or highly charged cations (e.g. Sn^{4+} or Zr^{4+}).

3.6. Molecular dynamics simulation of the Be(II) uptake by C–S–H

The structural properties (coordination numbers and ion-ion distances) of hydrated beryllium ion in solution are reported in several theoretical and computational studies (Asthağiri and Pratt, 2003;

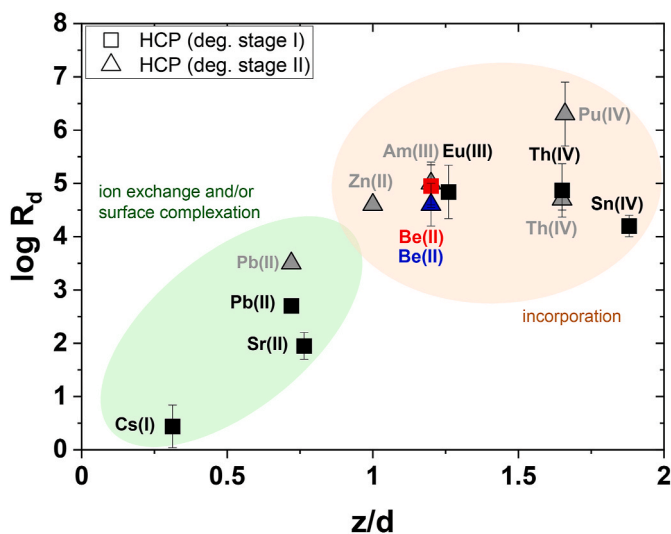


Fig. 6. Modification of the figure originally reported in Wieland and Van Loon (2003) for the uptake of different metal ions by HCP (deg. stage I) as a function of the z/d ratio. The original figure has been updated with data for Be(II) (HCP in deg. stage II and I; this work; Çevirim-Papaioannou et al. (2021)), Pb(II) (HCP deg. stage I and II; Wieland, 2014), Zn(II) (C–S–H at pH = 12.5; Ziegler et al., 2001a,b), Am(III) (HCP deg. stage II; Pointeau et al., 2004a,b), Th(IV) (HCP deg. stage II; Pointeau et al., 2004a,b) and Pu(IV) (HCP deg. stage II; Tasi et al., 2021).

Raymond et al., 2020; Rozmanov et al., 2004; Rudolph et al., 2009). It is known that the Be^{2+} aqua complex has a preferred tetrahedral geometry, with an average Be–O_w distance of 0.164–0.167 nm (Azam et al., 2009; Smirnov et al., 2008). The calculated radial distribution functions and running coordination numbers for Be–O, Be–Ca, and Be–Be pairs in the studied interface can be found in Fig. SD-3 in the Supplementary Data.

Atomic density profiles next to the (001) surface of C–S–H are presented in Fig. 7 (a). It is well-known that Ca^{2+} is strongly attracted to the deprotonated negatively charged surface and forms a layer that at high Ca^{2+} concentration inverts the overall surface charge from negative to positive (Pointeau et al., 2006; Viallis-Terrisse et al., 2001). There are several possible binding geometries for Ca^{2+} with C–S–H silanol groups, therefore, a series of overlapped peaks of Ca^{2+} is found at a close distance from the surface. The highest peak at 0.15 nm corresponds to inner-sphere coordination with 2 silanol groups. Beryllium is found farther from the C–S–H surface, and the density profile is showing two distinct peaks: at the distance ranges of 0.30–0.52 nm and 0.53–0.70 nm. There is a maximum density of aqueous hydroxyl (OH^-) between adsorbed Ca^{2+} and Be^{2+} (0.25–0.35 nm). Partially these hydroxyls belong to Ca^{2+} -OH pairs, and partially to Ca^{2+} -Be(OH)₃ and Ca^{2+} -Be(OH)₄⁻ adsorbed on the surface. As a result, the sorption of beryllium is observed not through the direct binding, but mostly through Ca-bridges (both coordination with surface Ca^{2+} and sorption of Ca–Be complexes from the solution is possible).

The formed complexes were stable during the production simulation time, which allowed us to identify them more accurately with the help of time-averaged 2D surface maps. The contour density maps and the surface complexes of beryllium are shown in Fig. 7 (b).

Beryllium is known to have a very ordered second coordination sphere. It was found that aqueous beryllium hydroxides can coordinate multiple Ca^{2+} cations of the C–S–H surface, forming potentially a much stronger surface complex. Three most stable inner-sphere (IS) complexes were identified (Fig. 8): IS-1 ($\text{Ca}_2\text{Be}(\text{OH})_3$ bound to 3 deprotonated silanol groups), IS-2 ($\text{CaBe}(\text{OH})_3$ bound to 2 deprotonated silanol groups), and IS-3 ($\text{Ca}_3\text{Be}(\text{OH})_4$ coordinated with 3 deprotonated silanol groups). These complexes correspond to the first beryllium maximum of the 1D density profile.

Additionally, a stable outer-sphere complex (OS-1) was observed with water molecules present between Ca^{2+} and the surface that corresponds to the second maximum of the profile. Sorption of hydroxocomplexes on C–S–H through Ca bridging has been already seen for uranyl (Androniuk et al., 2019), and this uptake mechanism could be expected for other divalent cations.

As discussed in Section 3.2, the adsorption of Be(II) is not very fast, and the incorporation of Be^{2+} into the C–S–H structure is expected under equilibrium conditions. To be able to sample this kind of sorption, a different computational method will be used in the future to overcome the kinetic factor, e.g. umbrella sampling or replica MD. These calculations will consider also the C–S–H interlayer, which is expected to play a relevant role in the uptake of Be(II) and will be reported in a separate publication by Androniuk et al.

3.7. Conclusions

We have provided the first ever direct experimental evidence that Be(II) sorbs strongly in the cementitious systems investigated (HCP deg. stage II, low pH cement, C–S–H with Ca:Si = 0.6, 1.0 and 1.6). The similar uptake determined for cement and C–S–H phases confirms that the latter are the main sink of beryllium in cementitious materials. The kinetic behavior supported a two-step uptake mechanism, including a fast surface complexation process followed by the slower incorporation of Be(II) in C–S–H. The stronger uptake of Be(II) ($\log R_d \approx 7$) observed at pH ≈ 10 correlates with the predominance of the neutral species $\text{Be}(\text{OH})_2(\text{aq})$ in solution. Lower and nearly constant $\log R_d$ values are determined within $12 \leq \text{pH} \leq 13.2$, suggesting a similar uptake of the anionic species $\text{Be}(\text{OH})_3^-$ and $\text{Be}(\text{OH})_4^{2-}$. In contrast to this finding, a

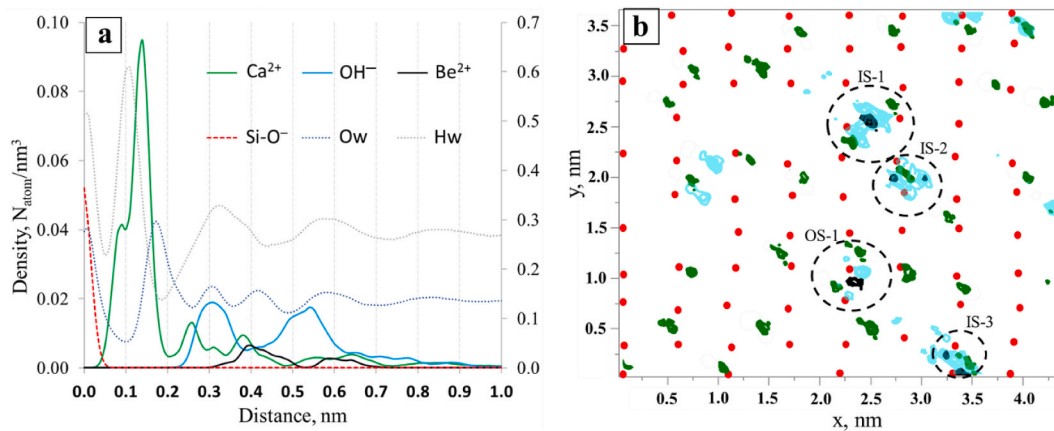


Fig. 7. (a) Atomic density profiles of solution species near the C–S–H surface. The right-side axis shows densities plotted with dotted lines. (b) Atomic density contour maps of time-averaged surface distributions of selected atoms at $d \approx 0.1\text{--}0.5$ nm from the surface.

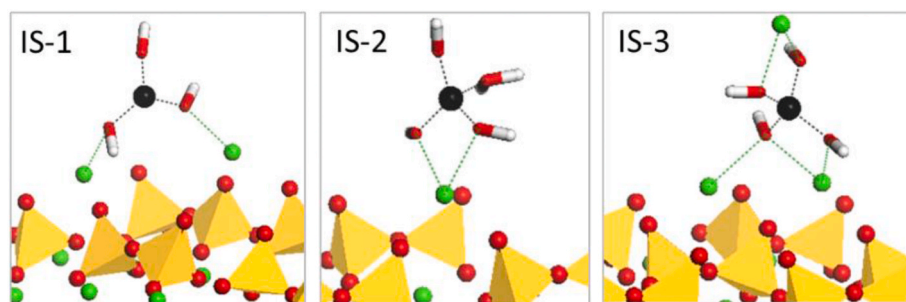


Fig. 8. The simulation snapshots of defined complexes (colour scheme: Si – yellow; Ca – green; O – red; H – white; Be – black). (For interpretation of the references to colour in this figure legend, the reader is referred to the Web version of this article.)

clear decrease in $\log R_d$ values is observed for the uptake of Be(II) by TiO_2 within the same pH-range. This supports that incorporation is the main uptake mechanism in cement/C–S–H phases, as opposed to the surface complexation mechanism controlling the uptake of Be(II) by TiO_2 .

Although the uptake of metal ions by cement and C–S–H phases is affected by several parameters (pH, metal speciation, [Ca], Ca:Si in the solid phase, etc.), it can be qualitatively explained by the charge-to-size ratio (z/d). This relationship satisfactorily explains the similar sorption observed for elements as different as Be(II) ($z/d = 1.2$), Zn(II) ($z/d = 1.0$), Eu(III) ($z/d = 1.13$) or Am(III) ($z/d = 1.2$) (Pointeau et al., 2004; Wieland and Van Loon, 2003; Ziegler et al., 2001).

Molecular dynamics highlight the key role of Ca in the uptake of Be(II) by C–S–H phases. Three main surface complexes have been identified: $>\text{Ca}_2\text{Be}(\text{OH})_3$ (bound to 3 deprotonated silanol groups), $>\text{CaBe}(\text{OH})_3$ (bound to 2 deprotonated silanol groups), and $>\text{Ca}_3\text{Be}(\text{OH})_4$ (coordinated with 3 deprotonated silanol groups). Molecular dynamics calculations have shown a great potential for the description of Be(II) uptake by the C–S–H surface, and future work at KIT-INE will target the description of processes taking place at the C–S–H interlayer, which is expected to play a relevant role in the uptake of Be(II) and other strongly sorbing metal ions.

This work provides a comprehensive quantitative and mechanistic description of the uptake of beryllium by cementitious material which so far was considered negligible in the view of lacking experimental studies. This new information is of high relevance and allows to better quantify the retention of beryllium in the context of the Safety Case for deep underground repositories for nuclear waste. It provides also a thorough scientific basis for the future development of more detailed thermodynamic/geochemical models, e.g. in the form of aqueous-solid solution models.

Declaration of competing interest

The authors declare that they have no known competing financial interests or personal relationships that could have appeared to influence the work reported in this paper.

Acknowledgements

The research leading to these results has received funding from the European Union's European Atomic Energy Community's (Euratom) Horizon 2020 Programme (NFRP-2014/2015) under grant agreement, 662147 – Cebama. The research stay of S. Han at KIT-INE was partially funded through the Korea Nuclear International Cooperation Foundation (KONICOF) Nuclear Global Internship Program and the National Research Foundation of Korea funded by the Ministry of Education (NRF-2017M2B2B1072374).

Frank Geyer, Annika Kaufmann, Cornelia Walschburger and Melanie Bottle (all KIT-INE) are gratefully acknowledged for the ICP–MS/OES measurements and technical support. Thanks are due to Agost Gyula Tasi (KIT-INE) and Vanessa Montoya (currently UFZ) for the support with the preparation of the cement powder and fruitful discussions on the cement-RN systems. Klas Kallstrom (Swedish Nuclear Fuel and Waste Management Company, SKB) is kindly acknowledged for providing one of the cement rods used in this study. The authors wish to thank Francis Claret (BRGM) for his help with the exchange of C–S–H phases with KIT-INE. Expert advice provided by Erich Wieland (PSI-LES) and Horst Geckeis (KIT-INE) throughout the development of this project is greatly appreciated.

Appendix A. Supplementary data

Supplementary data to this article can be found online at <https://doi.org/10.1016/j.chemosphere.2021.131094>.

Credit author statement

N. Çevirim-Papaioannou: Methodology, Investigation, Writing – original draft, Writing – review & editing, I. Androniuk: Methodology, Writing – original draft, Writing – review & editing, S. Han: Investigation, N. Ait Mouheb: Investigation, S. Gaboreau: Resources, W. Um: Writing – review & editing, X. Gaona: Conceptualization, Writing – review & editing, Supervision, Project administration, M. Altmaier: Writing – review & editing, Project administration, Funding acquisition

References

- Ait-Mouheb, N., 2021. Radionuclides Migration in the Low-pH Cement/clay Interface. PhD thesis, University of Jena, Germany.
- Ait Mouheb, N., Montoya, V., Schild, D., Soballa, E., Adam, C., Geyer, F., Schafer, T., 2019. Characterization and sorption properties of low pH cements. In: Altmaier, M., Montoya, V., Valls, A. (Eds.), *Proceeding of the Second Workshop of the Horizon 2020 CEBAMA Project*. KIT scientific publishing, Karlsruhe, pp. 29–39.
- Androniuk, I., Kalinichev, A.G., 2020. Molecular dynamics simulation of the interaction of uranium (VI) with the C-S-H phase of cement in the presence of gluconate. *Appl. Geochem.* 113.
- Androniuk, I., Landesman, C., Henocq, P., Kalinichev, A.G., 2017. Adsorption of gluconate and uranyl on C-S-H phases: combination of wet chemistry experiments and molecular dynamics simulations for the binary systems. *Phys. Chem. Earth* 99, 194–203.
- Asthağiri, D., Pratt, L.R., 2003. Quasi-chemical study of $\text{Be}^{2+}(\text{aq})$ speciation. *Chem. Phys. Lett.* 371 (5–6), 613–619.
- Atkins, M., Glasser, F.P., 1992. Application of Portland cement-based materials to radioactive waste immobilization. *Waste Manage* 12 (2–3), 105–131.
- Atkinson, A., Everitt, N., Guppy, R., 1988. Evolution of pH in a rad-waste repository: internal reactions between concrete constituents. UKAEA Report, AERE-R12939, Harwell, UK.
- Azam, S.S., Hofer, T.S., Bhattacharjee, A., Lim, L.H.V., Pribil, A.B., Randolph, B.R., Rode, B.M., 2009. Beryllium(II): the strongest structure-forming ion in water? A QMCF MD simulation study. *J. Phys. Chem. B* 113 (27), 9289–9295.
- Barzgar, S., Lothenbach, B., Tarik, M., Di Giacomo, A., Ludwig, C., 2020. The effect of sodium hydroxide on Al uptake by calcium silicate hydrates (C-S-H). *J. Colloid Interface Sci.* 572, 246–256.
- Bayless, S., Ewart, F.T., Howse, R.M., Lane, S.A., Pilkington, N.J., Smith-Briggs, J.L., Willmams, S.J., 1989. The solubility and sorption of radium and tin in a cementitious near-field environment. *Mater. Res. Soc. Symp. Proc.* 127, 879–885.
- Beeston, J.M., 1970. Beryllium metal as a neutron moderator and reflector material. *Nucl. Eng. Des.* 14 (3), 445.
- Bernard, E., Dauzères, A., Lothenbach, B., 2018a. Magnesium and calcium silicate hydrates, Part II: Mg-exchange at the interface “low-pH” cement and magnesium environment studied in a C-S-H and M-S-H model system. *Appl. Geochem.* 89, 210–218.
- Bernard, E., Lothenbach, B., Cau-Dit-Coumes, C., Chlique, C., Dauzères, A., Pochard, I., 2018b. Magnesium and calcium silicate hydrates, Part I: investigation of the possible magnesium incorporation in calcium silicate hydrate (C-S-H) and of the calcium in magnesium silicate hydrate (M-S-H). *Appl. Geochem.* 89, 229–242.
- Berner, U.R., 1992. Evolution of porewater chemistry during degradation of cement in a radioactive waste repository environment. *Waste Manage* 12, 201–219.
- Bouby, M., Lutzenkirchen, J., Dardenne, K., Preocanin, T., Denecke, M.A., Klenze, R., Geckeis, H., 2010. Sorption of Eu(III) onto titanium dioxide: measurements and modeling. *J. Colloid Interface Sci.* 350 (2), 551–561.
- Bruno, J., González-Siso, M.R., Duro, L., Gaona, X., Altmaier, M., 2018. Key Master Variables Affecting the Mobility of Ni, Pu, Tc and U in the Near Field of the SFR Repository. Main Experimental Findings and PA Implications of the PhD Thesis, SKB Technical Report, 18-01. Svensk Kärnbränslehantering AB, Solna, Sweden.
- Bu, J., Teresa, R.G., Brown, K.G., Sanchez, F., 2019. Adsorption mechanisms of cesium at calcium-silicate-hydrate surfaces using molecular dynamics simulations. *J. Nucl. Mater.* 515, 35–51.
- Calvo, J.L.G., Hidalgo, A., Alonso, C., Luco, L.F., 2010. Development of low-pH cementitious materials for HLW repositories Resistance against ground waters aggression. *Cement Concr. Res.* 40 (8), 1290–1297.
- Çevirim-Papaioannou, N., Gaona, X., Bottle, M., Bethune Yalcintas, E., Schild, D., Adam, C., Sittel, T., Altmaier, M., 2020. Thermodynamic description of Be(II) solubility and hydrolysis in acidic to hyperalkaline NaCl and KCl solutions. *Appl. Geochem.* 117, 1–13.
- Çevirim-Papaioannou, N., Han, S., Androniuk, I., Um, W., Altmaier, M., Gaona, X., 2021. Uptake of Be(II) by cement CEM I in the degradation stage I: wet-chemistry and molecular dynamics studies. *Minerals*. Submitted for publication.
- Chandler, D., Primm, R.T., Maldonado, G.I., 2009. Reactivity Accountability Attributed to Beryllium Reflector Poisons in the High Flux Isotope Reactor. ORNL Report, TM-2009/188, Oak Ridge, USA.
- Churakov, S.V., Labbez, C., 2017. Thermodynamics and molecular mechanism of Al incorporation in calcium silicate hydrates. *J. Phys. Chem. C* 121 (8), 4412–4419.
- Codina, M., Cau-Dit-Coumes, C., Le Bescep, P., Verdier, J., Ollivier, J.P., 2008. Design and characterization of low-heat and low-alkalinity cements. *Cement Concr. Res.* 38 (4), 437–448.
- Cong, X.D., Kirkpatrick, R.J., 1996. Si-29 MAS NMR study of the structure of calcium silicate hydrate. *Adv. Cement Base Mater.* 3 (3–4), 144–156.
- Coumes, C.C.D., Courtois, S., Nectoux, D., Leclercq, S., Bourbon, X., 2006. Formulating a low-alkalinity, high-resistance and low-heat concrete for radioactive waste repositories. *Cement Concr. Res.* 36 (12), 2152–2163.
- Cygan, R.T., Liang, J.J., Kalinichev, A.G., 2004. Molecular models of hydroxide, oxyhydroxide, and clay phases and the development of a general force field. *J. Phys. Chem. B* 108 (4), 1255–1266.
- D’Incal, A., Hofer, T.S., Randolph, B.R., Rode, B.M., 2006. Be(II) in aqueous solution - an extended ab initio QM/MM MD study. *Phys. Chem. Chem. Phys.* 8 (24), 2841–2847.
- Dauzères, A., Le Bescep, P., Sardini, P., Coumes, C.C.D., 2010. Physico-chemical investigation of clayey/cement-based materials interaction in the context of geological waste disposal: experimental approach and results. *Cement Concr. Res.* 40 (8), 1327–1340.
- De, S., Sabu, G., Zacharias, M., 2020. Molecular mechanism of Be^{2+} -ion binding to HLA-DP2: tetrahedral coordination, conformational changes and multi-ion binding. *Phys. Chem. Chem. Phys.* 22 (2), 799–810.
- Gaboreau, S., Grangeon, S., Claret, F., Ihiwakrim, D., Ersen, O., Montouillout, V., Maubec, N., Roos, C., Henocq, P., Carteret, C., 2020. Hydration properties and interlayer organization in synthetic C-S-H. *Langmuir* 36 (32), 9449–9464.
- Gaona, X., Dahn, R., Tits, J., Scheinost, A.C., Wieland, E., 2011. Uptake of Np(IV) by C-S-H phases and cement paste: an EXAFS study. *Environ. Sci. Technol.* 45 (20), 8765–8771.
- Gnanakaran, S., Scott, B., McCleskey, T.M., Garcia, A.E., 2008. Perturbation of local solvent structure by a small dication: a theoretical study on structural, vibrational, and reactive properties of beryllium ion in water. *J. Phys. Chem. B* 112 (10), 2958–2963.
- Grangeon, S., Fernandez-Martinez, A., Baronnet, A., Marty, N., Poulain, A., Elkaim, E., Roos, D., Gaboreau, S., Henocq, P., Claret, F., 2017. Quantitative X-ray pair distribution function analysis of nanocrystalline calcium silicate hydrates: a contribution to the understanding of cement chemistry. *J. Appl. Crystallogr.* 50, 14–21.
- Guo, Z.J., Niu, L.J., Tao, Z.Y., 2005. Sorption of Th(IV) ions onto TiO_2 : effects of contact time, ionic strength, thorium concentration and phosphate. *J. Radioanal. Nucl. Chem.* 266 (2), 333–338.
- Hakem, N., Fourest, B., Guillaumont, R., Marmier, N., 1996. Sorption of iodine and cesium on some mineral oxide colloids. *Radiochim. Acta* 74, 225–230.
- Hausler, V., Amayri, S., Beck, A., Platte, T., Stern, T.A., Vitova, T., Reich, T., 2018. Uptake of actinides by calcium silicate hydrate (C-S-H) phases. *Appl. Geochem.* 98, 426–434.
- Holland, T.R., Lee, D.J., 1992. Radionuclide getters in cement. *Cement Concr. Res.* 22 (2–3), 247–258.
- Honorio, T., Benboujema, F., Bore, T., Ferhat, M., Vourc’h, E., 2019. The pore solution of cement-based materials: structure and dynamics of water and ions from molecular simulations. *Phys. Chem. Chem. Phys.* 21 (21), 11111–11121.
- Jamil, T., Javadi, A., Heinz, H., 2020. Mechanism of molecular interaction of acrylate-polyethylene glycol acrylate copolymers with calcium silicate hydrate surfaces. *Green Chem.* 22 (5), 1577–1593.
- Jenni, A., Mader, U., Lerouge, C., Gaboreau, S., Schwyn, B., 2014. In situ interaction between different concretes and Opalinus Clay. *Phys. Chem. Earth* 70–71, 71–83.
- Kalinichev, A.G., Wang, J.W., Kirkpatrick, R.J., 2007. Molecular dynamics modeling of the structure, dynamics and energetics of mineral-water interfaces: application to cement materials. *Cement Concr. Res.* 37 (3), 337–347.
- Kawamura, H., Tanaka, S., Ishitsuka, E., 2004. In: *Proceedings of the Sixth IEA International Workshop on Beryllium Technology for Fusion*, Miyazaki, Japan.
- Kirkpatrick, R.J., Kalinichev, A.G., Hou, X., Struble, L., 2005a. Experimental and molecular dynamics modeling studies of interlayer swelling: water incorporation in kanemite and ASR gel. *Mater. Struct.* 38 (278), 449–458.
- Kirkpatrick, R.J., Kalinichev, A.G., Wang, J., 2005b. Molecular dynamics modelling of hydrated mineral interlayers and surfaces: structure and dynamics. *Mineral. Mag.* 69 (3), 289–308.
- Kremleva, A., Kruger, S., Rosch, N., 2020. Uranyl(VI) sorption in calcium silicate hydrate phases. A quantum chemical study of tobermorite models. *Appl. Geochem.* 113.
- L’Hospital, E., Lothenbach, B., Le Saout, G., Kulik, D., Scrivener, K., 2015. Incorporation of aluminium in calcium-silicate-hydrates. *Cement Concr. Res.* 75, 91–103.
- Lange, S., Kowalski, P.M., Psenicka, M., Klinkenberg, M., Rohmen, S., Bosbach, D., Deissmann, G., 2018. Uptake of Ra-226 in cementitious systems: a complementary solution chemistry and atomistic simulation study. *Appl. Geochem.* 96, 204–216.
- Li, P.F., Merz, K.M., 2014. Taking into account the ion-induced dipole interaction in the nonbonded model of ions. *J. Chem. Theor. Comput.* 10 (1), 289–297.
- Li, Z., Song, L.F., Li, P., Merz Jr., K.M., 2020. Systematic parametrization of divalent metal ions for the OPC3, OPC, TIP3P-fb, and TIP4P-fb water models. *J. Chem. Theor. Comput.* 16 (7), 4429–4442.
- Longhurst, G.R., Carboneau, M.I., Mullen, C.K., S, J.W., 2003. Challenges for disposal of irradiated beryllium. In: *Proceedings of the 6th IEA Workshop on Beryllium Technology*, Dec. 2–5, Mizayaki, Japan.
- Lothenbach, B., Le Saout, G., Ben Haha, M., Figi, R., Wieland, E., 2012. Hydration of a low-alkali CEM III/B-SiO₂ cement (LALC). *Cement Concr. Res.* 42 (2), 410–423.
- Lothenbach, B., Nied, D., L’Hospital, E., Achiedo, G., Dauzères, A., 2015. Magnesium and calcium silicate hydrates. *Cement Concr. Res.* 77, 60–68.

- Mancini, A., Wieand, E., Geng, G., Lotenbach, B., Wehrli, B., Dahn, R., 2020. Fe(II) interaction with cement phases: method development, wet, chemical studies and X-ray absorption spectroscopy. *J. Colloid Interface Sci.* 588, 692–704.
- Mandaliev, P., Dahn, R., Tits, J., Wehrli, B., Wieland, E., 2010a. EXAFS study of Nd(III) uptake by amorphous calcium silicate hydrates (C-S-H). *J. Colloid Interface Sci.* 342 (1), 1–7.
- Mandaliev, P., Wieland, E., Dahn, R., Tits, J., Churakov, S.V., Zaharko, O., 2010b. Mechanisms of Nd(III) uptake by 11 angstrom tobermorite and xonotlite. *Appl. Geochem.* 25 (6), 763–777.
- Mishra, R.K., Mohamed, A.K., Geissbuhler, D., Manzano, H., Jamil, T., Shahsavari, R., Kalinichev, A.G., Galmardini, S., Tao, L., Heinz, H., Pelleng, R., van Duin, A.C.T., Parker, S.C., Flatt, R.J., Bowen, P., 2017. cemff: a force field database for cementitious materials including validations, applications and opportunities. *Cement Concr. Res.* 102, 68–89.
- Missana, T., Garcia-Gutierrez, M., Mingarro, M., Alonso, U., 2017. Analysis of barium retention mechanisms on calcium silicate hydrate phases. *Cement Concr. Res.* 93, 8–16.
- Monteiro, P.J.M., Geng, G.Q., Marchon, D., Li, J.Q., Alapati, P., Kurtis, K.E., Qomi, M.J.A., 2019. Advances in characterizing and understanding the microstructure of cementitious materials. *Cement Concr. Res.* 124.
- Mutisya, S.M., de Almeida, J.M., Miranda, C.R., 2017. Molecular simulations of cement based materials: a comparison between first principles and classical force field calculations. *Comput. Mater. Sci.* 138, 392–402.
- Ochs, M., Dirk, M., Wang, L., 2016. Radionuclide and Metal Sorption on Cement and Concrete. Springer, Switzerland.
- Ochs, M., Talerico, C., Lothenbach, B., 2002. Systematic trends and empirical modeling of lead uptake by cements and cement minerals. *Mater. Res. Soc. Symp. Proc.* 757, 101.
- Olmeda, J., Missana, T., Grandia, F., Grive, M., Garcia-Gutierrez, M., Mingarro, M., Alonso, U., Colas, E., Henocq, P., Munier, I., Robinet, J.C., 2019. Radium retention by blended cement pastes and pure phases (C-S-H and C-A-S-H gels): experimental assessment and modelling exercises. *Appl. Geochem.* 105, 45–54.
- Pointeau, I., Landesman, C., Giffaut, E., Reiller, P., 2004a. Reproducibility of the uptake of U(VI) onto degraded cement pastes and calcium silicate hydrate phases. *Radiochim. Acta* 92 (9–11), 645–650.
- Pointeau, I., Landesman, C., Giffaut, E., Reiller, P., Coreau, N., Moisan, C., Reiller, P., 2004b. Etude de la rétention chimique des radionucléides Cs(I), Am(III), Zr(IV), Pu(IV), Nb(V), U(VI) et Tc(IV) par des matériaux cimentaires dégradés. In: Rapport Technique RT DPC/SECR 03-037. CEA, Saclay, France.
- Pointeau, I., Marmier, N., Fromage, F., Fedoroff, M., Giffaut, E., 2001a. Cesium and Lead uptake by CSH phases of hydrated cement. *Mater. Res. Soc. Symp. Proc.* 663, 105–113.
- Pointeau, I., Piriou, B., Fedoroff, M., Barthes, M.G., Marmier, N., Fromage, F., 2001b. Sorption mechanisms of Eu^{3+} on CSH phases of hydrated cements. *J. Colloid Interface Sci.* 236 (2), 252–259.
- Pointeau, I., Reiller, P., Mace, N., Landesman, C., Coreau, N., 2006. Measurement and modeling of the surface potential evolution of hydrated cement pastes as a function of degradation. *J. Colloid Interface Sci.* 300 (1), 33–44.
- Pomies, M.P., Lequeux, N., Boch, P., 2001. Speciation of cadmium in cement Part I. Cd^{2+} uptake by C-S-H. *Cement Concr. Res.* 31 (4), 563–569.
- Raymond, O., Buhl, M., Lane, J.R., Henderson, W., Brothers, P.J., Plieger, P.G., 2020. Ab initio molecular dynamics investigation of beryllium complexes. *Inorg. Chem.* 59 (4), 2413–2425.
- Roosz, C., Vieillard, P., Blanc, P., Gaboreau, S., Gailhanou, H., Braithwaite, D., Montouillout, V., Denoyel, R., Henocq, P., Made, B., 2018. Thermodynamic properties of C-S-H, C-A-S-H and M-S-H phases: results from direct measurements and predictive modelling. *Appl. Geochem.* 92, 140–156.
- Rozmanov, D.A., Sizova, O.V., Burkov, K.A., 2004. Ab initio studies of the beryllium aquahydroxocomplexes. *J. Mol. Struct-Theochem.* 712 (1–3), 123–130.
- Rudolph, W.W., Fischer, D., Irmer, G., Pye, C.C., 2009. Hydration of beryllium(II) in aqueous solutions of common inorganic salts. A combined vibrational spectroscopic and ab initio molecular orbital study. *Dalton Trans.* (33), 6513–6527.
- Savage, D., Benbow, S.J., 2007. Low pH Cements, SKI Report, 2007:32. Swedish Nuclear Power Inspectorate, Stockholm, Sweden.
- Schlegel, M.L., Pointeau, I., Coreau, N., Reiller, P., 2004. Mechanism of europium retention by calcium silicate hydrates: an EXAFS study. *Environ. Sci. Technol.* 38 (16), 4423–4431.
- Schmidt, J., Vogelsberger, W., 2009. Aqueous long-term solubility of titania nanoparticles and titanium(IV) hydrolysis in a sodium chloride system studied by adsorptive stripping voltammetry. *J. Solut. Chem.* 38 (10), 1267–1282.
- Smirnov, P.R., Trostin, V.N., 2008. Structural parameters of hydration of Be^{2+} and Mg^{2+} ions in aqueous solutions of their salts. *Russ. J. Gen. Chem.* 78 (9), 1643–1649.
- Stumpf, T., Tits, J., Walther, C., Wieland, E., Fanghanel, T., 2004. Uptake of trivalent actinides (curium(III)) by hardened cement paste: a time-resolved laser fluorescence spectroscopy study. *J. Colloid Interface Sci.* 276 (1), 118–124.
- Tasi, A., 2018. Solubility, Redox and Sorption Behavior of Plutonium in the Presence of α -D-isosaccharinich Acid Cement under Reducing Conditions. PhD thesis. Karlsruhe Institute for Technology, Germany.
- Tasi, A., Gaona, X., Rabung, T., Fellhauer, D., Rothe, J., Dardenne, K., Lutzenkirchen, J., Grive, M., Colas, E., Bruno, J., Kallstrom, K., Altmaier, M., Geckeis, H., 2021. Plutonium retention in the isosaccharinate - cement system. *Appl. Geochem.* 126.
- Taylor, H.F.W., 1997. *Cement Chemistry*, second ed. Thomas Telford, London.
- Thorne, M.C., 2007. *A Guide to the Spreadsheet Model Used for Groundwater and Well Calculations for Generic Performance Assessments*, Limited Report to United Kingdom Nirex, MTA/P0011C/206-4: Issue 2. Mike Thorne and Associates Limited, West Yorkshire, United Kingdom.
- Tits, J., Gaona, X., Laube, A., Wieland, E., 2014. Influence of the redox state on the neptunium sorption under alkaline conditions: batch sorption studies on titanium dioxide and calcium silicate hydrates. *Radiochim. Acta* 102 (5), 385–400.
- Tits, J., Geipel, G., Mace, N., Eilzer, M., Wieland, E., 2011. Determination of uranium(VI) sorbed species in calcium silicate hydrate phases: a laser-induced luminescence spectroscopy and batch sorption study. *J. Colloid Interface Sci.* 359 (1), 248–256.
- Tits, J., Iijima, K., Wieland, E., Kamei, G., 2006a. The uptake of radium by calcium silicate hydrates and hardened cement paste. *Radiochim. Acta* 94 (9–11), 637–643.
- Tits, J., Walther, C., Stumpf, T., Mace, N., Wieland, E., 2015. A luminescence line-narrowing spectroscopic study of the uranium(VI) interaction with cementitious materials and titanium dioxide. *Dalton Trans.* 44 (3), 966–976.
- Tits, J., Wieland, E., 2018. Actinide Sorption by Cementitious Materials. PSI technical report, 18-02. Paul Scherrer Institute, Villigen, Switzerland.
- Tits, J., Wieland, E., Muller, C.J., Landesman, C., Bradbury, M.H., 2006b. Strontium binding by calcium silicate hydrates. *J. Colloid Interface Sci.* 300 (1), 78–87.
- Tommaseo, C.E., Kersten, M., 2002. Aqueous solubility diagrams for cementitious waste stabilization systems. 3. Mechanism of zinc immobilization by calcium silicate hydrate. *Environ. Sci. Technol.* 36 (13), 2919–2925.
- Vasconcelos, R.G.W., Walkley, B., Day, S., Tang, C.C., Paraskevoulakos, H., Gardner, L.J., Corkhill, C.L., 2020. 18-month hydration of a low-pH cement for geological disposal of radioactive waste: the Cebama reference cement. *Appl. Geochem.* 116.
- Vehmas, T., Montoya, V., Alonso, M.C., Vasicek, R., Rastrick, E., Gaboreau, S., Vecernik, P., Leivo, M., Holt, E., Fink, N., Mouheb, N.A., Svoboda, J., Read, D., Cervinka, R., Vasconcelos, R., Corkhill, C., 2020. Characterization of Cebama low-pH reference concrete and assessment of its alteration with representative waters in radioactive waste repositories. *Appl. Geochem.* 121.
- Vialli-Terrisse, H., Nonat, A., Petit, J.C., 2001. Zeta-potential study of calcium silicate hydrates interacting with alkaline cations. *J. Colloid Interface Sci.* 244 (1), 58–65.
- Walsh, K.A., 2009. In: Olson, D.L., Vidal, E.E., Dalder, E., Goldberg, A., Mishra, B. (Eds.), *Beryllium Chemistry and Processing*. ASM international, Ohio, USA, pp. 20–26.
- Wieland, E., 2014. Sorption Data Base for the Cementitious Near Field of L/ILW and ILW Repositories for Provisional Safety Analyses for SGT-E2. Nagra Technical Report 14-08. Paul Scherrer Institut, Villigen, Switzerland.
- Wieland, E., Tits, J., Kunz, D., Daehn, R., 2008. Strontium uptake by cementitious materials. *Environ. Sci. Technol.* 42 (2), 403–409.
- Wieland, E., Van Loon, L., 2003. Cementitious Near-Field Sorption Data Base for Performance Assessment of an ILW Repository in Opalinus Clay. Technical Report 03-06. Paul Scherrer Institut, Villigen, Switzerland.
- Wilson, J., Thorne, M., Towler, G., 2009. *Treatment of Chemotoxic Species: (1) Quantitative Human Health Risk Assessment, QRS-1378M-1 Version 1.1*. Quintessa Limited, Oxfordshire, United Kingdom.
- Ziegler, F., Giere, R., Johnson, C.A., 2001a. Sorption mechanisms of zinc to calcium silicate hydrate: sorption and microscopic investigations. *Environ. Sci. Technol.* 35 (22), 4556–4561.
- Ziegler, F., Scheidegger, A.M., Johnson, C.A., Dahn, R., Wieland, E., 2001b. Sorption mechanisms of zinc to calcium silicate hydrate: X-ray absorption fine structure (XAFS) investigation. *Environ. Sci. Technol.* 35 (7), 1550–1555.